ISSN 1974-9821
Vol. 8 N. 2
April 2015

International Review on Modelling and Simulations (IREMOS)

Contents:

(continued on inside back cover)

Praise Worthy Prize

International Review on Modelling and Simulations (IREMOS)

Editor-in-Chief:

Santolo Meo
Department of Electrical Engineering
FEDERICO II University
21 Claudio - I80125 Naples, Italy
santolo@unina.it

The ***International Review on Modelling and Simulations (IREMOS)*** is a publication of the **Praise Worthy Prize S.r.l.**.
The Review is published bimonthly, appearing on the last day of February, April, June, August, October, December.

Published and Printed in Italy by **Praise Worthy Prize S.r.l.,** Naples, April 30, 2015.

International Review on Modelling and Simulations (I.RE.MO.S.), Vol. 8, N. 2
ISSN 1974-9821 April 2015

Improvement of Hydrogeological Models: a Case Study

A. Spalvins, J. Slangens, I. Lace, O. Aleksans, K. Krauklis

Abstract – *A case study on improvement of hydrogeological models (HM) is reported where HM of Latvia LAMO is considered. HM has been developed in 2010 – 2012 by scientists of Riga Technical University (RTU). LAMO has generalized geological and hydrogeological information that has been accumulated by the Latvian Environment, Geology and Meteorology Centre (LEGMC).*
In 2013 – 2014, LAMO has been considerably upgraded. Due to these upgrades, large amount of real hydrogeological and geological data has been added that have increased credibility of LAMO results. Essence of the main innovations is described and the next improvements of HM are considered. The case of LAMO improvement may be of interest for developers of large and complex hydrogeological models.

***Keywords**: Hydrogeological Model, Hydrographical Network, Numerical Interpolation, Transmissivity of Aquifers, Latvia*

Nomenclature

x, y, z	Cartesian coordinates for 3-dimensional space
h	Plane step used by the finite difference approximation on HM grid
u	Number of layers in HM grid
i	Number in turn of i-th layer
m	Thickness of geological layer
m_i	Thickness of i-th layer
k	Permeability of geological layer
k_i	Permeability of i-th layer
z_{i-1}, z_i	Elevations of i-th layer top and bottom surfaces
$z_{i-0.5}$	Elevation of surface where HM elementary block centers of i-th layer are located
z_0	Elevation of HM top surface
φ	Vector of piezometric head which components are found in nodes of HM grid
φ_i	Vector of piezometric head (part of φ) of i-th layer
ψ	Vector of boundary conditions for piezometric head
ψ_{river}, ψ_{lakes}	Vectors of boundary conditions (part of ψ) for rivers and lakes
β	Vector of boundary conditions for flows
A	Matrix of hydraulic conductivities for links of HM grid
A_{xy}, A_z	Matrixes (part of A) that represent horizontal and vertical links of HM grid
a_{xy}, a_z	Elements of A_{xy} and A_z
G	Matrix (part of A) that assembles links connecting nodes of HM grid with boundary conditions ψ
G_{river}, G_{lakes}	Matrixes (part of G) that assemble links connecting nodes of HM grid with boundary conditions ψ_{river} and ψ_{lakes}
q	Vector of groundwater flow
q_{river}, q_{lakes}	Vectors (part of q) of river and lake flows
q_{inflow}	Vector of inflow for flow balance module
q_{border}, q_{wells}	Vectors of flows for outer boundaries and discharge wells of flow balance module
S	Drawdown of groundwater head
T	Transmissivity of geological layer
R, r	Radiuses of well depression cone and its screen
l	Length of well screen
B	Leakage factor of aquifer
L	Area of layer
n	Number of grid nodes in m>0 area of a layer
σ	Interpolated value of pointwise data
τ_i	Weight of pointwise data σ_i
d_{0i}	Distance between grid node 0 and data locus of σ_i
p	Weighting power for interpolation method "inverse distance to power"

Units

meter	$m, m_i, l, S, R, r, B, d_{0i}, h, x, y$
meter^2	L
meters above sea level	$\varphi, \psi, \psi_{river}, \psi_{lakes}, z, z_{i-1}, z_i, z_{i-0.5}$ z_0
meter/day	k, k_i
meter^2/day	$T, A, A_{xy}, A_z, G, G_{river}, G_{lakes}, a_{xy}, a_z$
meter^3/day	$Q, \beta, q, q_{river}, q_{lakes}, , q_{border}, q_{wells}$
mm/year	$\gamma, \gamma_{i,i+1}$
litre/(sec meter)	v
no dimension	$u, \xi, \delta, n, \tau_i, p, i$

I. Introduction

The European Union (EU) countries are developing HM where, by means of computer modelling, the information is obtained for water resources management that must implement the EU aims defined in the Water Framework Directive 2000 [1]. In Latvia, the LEGMC team is preparing and updating the water resources management plans for cross-border type river basins districts: those of Venta, Lielupe, Daugava and Gauja rivers. In 2010-2012, HM LAMO has been established by scientists of RTU. LAMO simulates steady state average hydrogeological situation of Latvia. The land territory of Latvia and the area of the Gulf of Riga constitute the HM active area (Fig. 1). LAMO simulates 27 geological layers (Fig. 2). The commercial program Groundwater Vistas (GV) is used for running LAMO [2].

In [3], methods used to create LAMO have been explained and they are not described in this paper. In 2013, by using results of LAMO, scientists of RTU have prepared materials that are being applied by specialists of LEGMC. The main items of these materials are summarized in [4]. In 2013-2014, LAMO has been considerably updated [5]. Due to these innovations, at present, four successive versions of LAMO can be marked (Table I). These HM versions materialize the following LAMO upgrading plan that has been caused by analysis of the first incomplete results of LAMO [6] and by insight into the art of HM perfecting:

1. to correct HM for the northern part of Latvia, the thick united D2ar# aquifer must be split into smaller layers that in nature compose this aquifer;
2. to improve modelling of riversides and of the river flow regimes, valleys of rivers have to be fully incised into the HM body;
3. to reduce uncertainty of the HM results, the transmissivity maps of aquifers must be refined by using field data that can be provided by well pumping tests;
4. to ensure plausible modelling of groundwater interaction with rivers and lakes, their number in HM must be increased;
5. to simulate more exactly the much denser hydrographic network (rivers, lakes), the HM plane approximation step must be reduced from 500 meters to 250 meters;
6. to finalize the HM development, measurements of the river flows must be accounted for, because then the interaction between groundwater bodies and the rivers will be modelled more reliantly.

These six upgrades are focused on installing into HM as much real data, as possible, in order to increase its credibility. Each next improvement is more complex than the previous one. In 2013, the first very necessary upgrades (1 and 2) were applied, to alter the base version LAMO1 into LAMO2. At present, its results are used in practice. In 2014, the more complex innovations (3 and 4) have turned LAMO2 into LAMO3.

The version is transitory, hence it only prepares HM for implementing the last two decisive upgrades.

Fig. 1. Location of LAMO

No of HM plane		Name of layer	Geolo-gical code	HM plane code
1.		Relief	relh	relh
2.		Aeration zone	aer	aer
3.		Unconfined Quaternary	Q4-3	Q2
4.		Upper moraine	gQ3	gQ2z
5.		Confined Quaternary or Jura	Q1-3 J	Q1#
6.		Lower moraine or Triass	gQ1-3 T	gQ1#z
7.		Perma Karbons Skerveles Ketleru	P2 C1 D3šķ D3ktl	D3ktl#
8.		Ketleru	D3ktl	D3ktlz
9.		Zagares Svetes Tervetes Muru	D3žg D3sv D3tr D3mr	D3zg#
10.		Akmenes	D3ak	D3akz
11.		Akmenes Kursas Jonisku	D3ak D3krs D3jn	D3krs#
12.		Elejas Amulas	D3el D3aml	D3el#z
13.		Stipinu Katlesu Ogres Daugavas	D3stp D3ktl D3og D3dg	D3dg#
14.		Daugavas Salaspils	D3dg D3slp	D3slp#z
15.		Plavinu	D3pl	D3pl
16.		Plavinu Amatas	D3pl D3am	D3am#z
17.		Amatas	D3am	D3am
18.		Upper Gauja	D3gj2	D3gj2z
19.		Upper Gauja	D3gj2	D3gj2
20.		Lower Gauja	D3gj1	D3gj1z
21.		Lower Gauja	D3gj1	D3gj1
22.		Burtnieku	D2brt	D2brtz
23.		Burtnieku	D2brt	D2brt
24.		Arikula	D2ar	D2arz
25.		Arikula	D2ar	D2ar
26.		Narvas Narvas	D2nr2 D2nr1	D2nr#z
27.		Pernavas	D2prn	D2pr

- aquitard

-united aquifer; #z – united aquitard

Fig. 2. Vertical schematization of LAMO

TABLE I
VERSIONS OF LAMO

Name of version	Year of dispose	Approximation grid			Rivers in model			Lakes
		Plane step [meter]	Number of grid planes	Number of cells [$\times 10^6$]	Number	Valleys incised	Flow data used	Number
LAMO1	2012	500	25	14.25	199	no	no	67
LAMO2	2013	500	27	15.43	199	yes	no	67
LAMO3	2014	500	27	15.43	469	yes	no	127
LAMO4	2015	250	27	61.56	469	yes	yes	127

In 2015, the final upgrades (5 and 6) will create the most advanced LAMO4 version that will include the all applied upgrades. For LAMO, the residual (difference between monitored and simulated piezometric head values) does not exceed 1.7 meter (quadratic error) and 2% (relative error). Reliance of HM depends not only on the excellent residuals, but mainly on feasible modelling of groundwater flows and of their interaction with the hydrographical network. By putting into effect the upgrades 4, 5, 6 these processes for Latvia will be simulated more trustworthy.

For LAMO4, the tools MODPATH and MT3D of the GV system [2] will be applied, accordingly, for particle tracking and for modelling content of groundwater ingredients. Geochemical processes will be investigated and extra calibration of HM will be possible.

In the paper, mainly the LAMO2 and LAMO3 versions are described and compared, because they differ significantly in density of their hydrographical networks.

II. Mathematical Formulations

To describe upgrades of LAMO, some mathematical knowledge must be applied. By using the 3D-finite difference approximation, the x, y, z – grid of HM is built. The grid consists of ($h \times h \times m$) sized blocks (h is the block plane step, m is the variable thickness of a geological layer). For LAMO, h = 500 meters.

The model constitutes a rectangular u-tiered xy-layer system where u is the number of geological layers. For LAMO, u = 27 (Fig. 2). It is shown in Fig. 3 and Fig. 4 that most of the primary layers are outcropping. After emerging at the surface, such layers have the zero thickness m = 0. To avoid in GV calculations "the division by zero", m = 0 must replaced by small ε > 0 (for LAMO, ε = 0.02 meter).

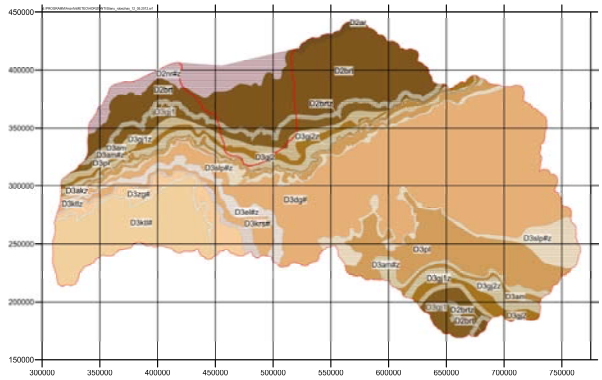

Fig. 3. Boundaries of primary geological strata

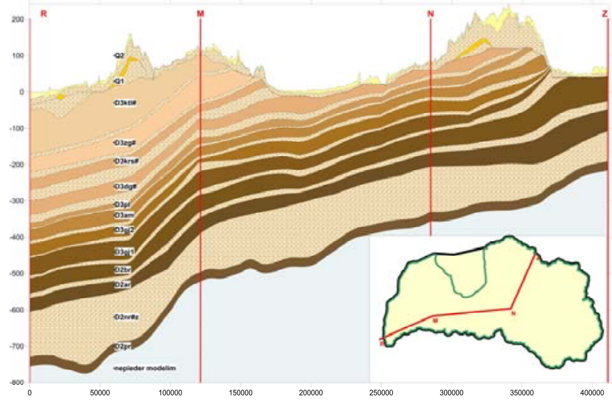

Fig. 4. Geological cross section

LAMO provides the 3D-distribution of piezometric head vector φ as the numerical solution of the boundary field problem which is approximated in nodes of the HM xyz–grid by the following algebraic expression:

$$A\varphi = \beta - G\psi, \quad A = A_{xy} + A_z \tag{1}$$

where A is the geological environment matrix which contains horizontal (A_{xy} – transmissivity T) and vertical (A_z – vertical hydraulic conductivity) elements of the HM grid; ψ and β are the boundary head and flow vectors, respectively; G is the diagonal matrix (part of A) assembled by elements linking the nodes where φ must be found with the nodes and points where ψ is given.

The vectors ψ and β represent the boundary conditions of the first and the second kind, respectively. For LAMO, the β–flow vector is presented only by discharges of water supply wells. To accelerate convergence of iterative solution process of the very large system (1), the ψ–type boundary conditions are applied on the exterior surfaces (top, bottom, sides) of the HM active body.

The boundary conditions ψ_{river} and ψ_{lakes} for rivers and lakes, accordingly, also enlarge the elements of G that ensure faster solution process of (1) [7]. The flows q_{riv} and q_{lakes} for rivers and lakes, accordingly, are simulated by the GV system, as follows:

$$q_{riv} = G_{riv}(\varphi - \psi_{riv}), \;\; q_{lakes} = G_{lakes}(\varphi - \psi_{lakes}) \tag{2}$$

where G_{riv} and G_{lakes} are diagonal matrixes (part of G) that assemble elements linking the boundary conditions ψ_{riv} and ψ_{lakes} with nodes of the HM grid. These elements control interaction of groundwater bodies with the rivers and lakes. To calibrate the interaction, the elements of G_{riv} and G_{lakes} must be adjusted.

The flows q_{riv} and q_{lakes} are interdependent with the groundwater head φ, their real values are not known.

Rough estimates for q_{riv} may provide measurements of river flows. Sometimes, it is assumed that q_{riv} represents the minimal observed river flow.

Because of the uncertainty of parameters that control the flows q_{riv} and q_{lakes} , the task of finding the true links G_{riv} and G_{lakes} is very complex. The elements a_{xy}, a_z of A_{xy}, A_z (or g_{xy}, g_z of G) are computed as follows:

$$a_{xy} = k\,m = T, \qquad a_z = h^2\, k_i / (m_i + m_{i+1}\, k_i / k_{i+1}) \qquad m_i = z_{i-1} - z_i \geq 0, \quad i = 1, 2, \ldots, u \qquad (3)$$

where z_{i-1}, z_i are elevations, accordingly, of the top and bottom surfaces of the i-th geological layer; z_0 represents the ground surface elevation ψ_{rel}-map; m_i, k_i are elements of digital m_i, k_i-maps of thickness and permeability of the i-th layer, accordingly; m_{i+1}, k_{i+1} are parameters of the next underlying plane of the HM grid. The set of z-maps describes the full geometry (stratification) of LAMO.

For the i-th layer, the HM grid block centres are located on the surface $z_{i-0.5}$:

$$z_{i-0.5} = 0.5(z_{i-1} + z_i), \qquad i = 1, 2, \ldots u \qquad (4)$$

The vector φ_i and the vertical infiltration flow $\gamma_{i,i+1}$ are spatially related to this surface. The flow $\gamma_{i,i+1}$ [mm/year] can be computed by using the formula:

$$\gamma_{i,i+1} = 0.73 \times 10^6 (\varphi_i - \varphi_{i+1})\, k_i / (m_i + m_{i+1}\, k_i / k_{i+1}) \qquad (5)$$

where the i-th and $(i+1)$-th layers are an aquitard and aquifer, respectively; $k_{i+1} >> k_i$; the units φ [meter asl], k [meter/day], m [meter] are applied.

The above section contains information that is important for the HM upgrades and it does not describe the methods used for creating of LAMO [3].

III. LAMO2 Upgrades

The concepts that turned LAMO1 into LAMO2 were initiated by knowledge provided by geological sections.

III.1. Geological Sections

The geological section map assembles the xy-type data φ and γ from the $z_{i-0.5}$ surfaces into the λz-picture that is projected on the geological stratification formation.

The map for a section provides worthy information of the φ and γ distributions that cannot easily deducted from their xy-type data. To create the φ or γ–map of a section , their interpolated data located on the middle lines $z_{i-0.5}$ of aquitards and aquifers, must be applied as the boundary conditions of the first kind for the Laplace's equation [8].

Its finite – difference solution on the λz–grid plane of the section represents its φ or γ –map. This method was developed by scientists of RTU. As an example of its apply, obtaining of the φ–map for a section of Fig. 5 is explained.

The arbitrary λz–grid of the size 200×600 was used; the grid steps h_λ =1000 meters, h_z =1.0 meter were applied to approximate the section longitude λ and its height z, respectively. The solution of this subsidiary problem (φ–map of Fig. 5) was provided by the GV system and drawn by SURFER [9]. In Fig. 5, any φ–isoline within an aquifer is vertical. This effect is due to smallness of the head difference between the top and bottom of an aquifer.

The head difference φ_i-φ_{i+1} = $\Delta_{i,i+1}$ = Δ_I + Δ_{i+1} divides between the vertical conductances a_i and a_{i+1} of an aquitard and aquifer, if $a_{i+1} >> a_i$ then:

$$\Delta_i = \Delta_{i,i+1}\, a_{i,i+1}/a_i \rightarrow \Delta_{i,i+1}, \quad \Delta_{i+1} = \Delta_{i,i+1}\, a_{i,i+1}/a_{i+1} \rightarrow 0 \qquad a_{i,i+1} = a_i\, a_{i+1} / (a_i + a_{i+1}) \qquad (6)$$

where $a_{i,i+1}$ are the a_z –links (mean harmonic of a_i and a_{i+1}) that connect the nodes of the neighbouring HM grid planes. It follows from (6) that, to keep Δ_{i+1} =0, the top and bottom surfaces z_i and z_{i+1} of the $(i+1)$-th aquifer, must be used for fixing the conditions φ_{i+1}.

To ensure verticality of isolines, in the λz-grid nodes that are located between these two surfaces, the conditions φ_{i+1} must also be fixed.

It is not necessary to use any special boundary conditions for the i-th aquitard, because on its top and bottom surfaces, the conditions for the neighbouring aquifers are set. Only the φ–distributions for the aquitards must be found, hence the aquifers carry the boundary conditions that keep the isolines vertical. .

In [6] that was based on results of LAMO1, the customary 2D xy–distributions for heads φ and flows γ appeared doubtless.

Review of the φ–maps of λz – cross sections revealed deficiencies of LAMO1 that needed to be corrected. As an example, the φ–map of Fig. 5 can be used. It suggested improvements that turned LAMO1 into LAMO2:

- to divert the unlikely even φ–distribution within the 23-th thick united aquifer D2ar#, the one was split into its natural parts: the aquifers D2brt, D2ar and the aquitard D2arz (Fig. 2); the number of LAMO planes increased from 25 to 27;
- to simulate the reversides and flows of rivers more correctly, valleys of rivers were fully incised into the HM body; for the early LAMO1 version, the valleys were immersed only into the Quaternary strata (see the river Gauja in Fig. 5).

In Fig. 6, the LAMO2 φ–map for the section 2W-2E is shown. It is obvious that the splitting of the united thick D2ar# aquifer was required, to improve HM for the northern part of Latvia. There only this aquifer represents the active groundwater zone of the primary layers and its top reaches the Quaternary strata (Fig. 3 and Fig. 4).

Due to presence of the D2arz aquitard, the φ–distributions for the D2brt and D2ar aquifers are quite different and more feasible, especially, for the recharge areas and for the discharge zone of the Gauja river.

It was also found in 2013, how the infiltration γ–maps for sections could be created by using the method that was applied for obtaining of the φ–maps.

To create the γ–maps for the sections, one have to assume that, within aquitards, the isolines of infiltration must be verticals and the infiltration redistributes within aquifers. To confirm practical applicability of these suppositions, one must estimate the ratio $\rho = q_{xy}/q_z$ of flows for the grid nodes of aquitards and aquifers:

$$\rho = (m_0 / h)^2 \text{ – for aquitards,}$$
$$\rho = (k / k_0)(m\, m_0 / h^2) \text{ - for aquifers} \quad (7)$$

where k_0, m_0; and k, m; $k >> k_0$ are parameters of aquitards and aquifers, accordingly. It follows from (7) that the ratio ρ is very small for aquitards and its value may be considerable for aquifers. Therefore, within aquitards for the section of the γ–flows, the isolines must be vertical, because there change of the flow q_z is insignificant, hence the lateral q_{xy} –flow is much smaller.

Therefore, the conditions for the γ isoline verticality must be fixed within the aquitards and the γ–distribution must be found for aquifers.

In Fig. 7, γ–map for the section 2W-2E is shown. Together with the isolines, the SURFER color fill mode is applied.

The γ–maps are very useful as tools for finding various faults of linking rivers and lakes with the HM body.

The ground surface ψ_{rel} controls the γ–flow on the HM top. Rivers and lowlands cause groundwater discharges, but the hilly areas are the recharge sources.

On the section, the both φ and γ–maps can be projected simultaneously [5].

III.2. Incisions of River Valleys

The weighty effect of river valley incisions can be partially observed for the river Gauja in Fig. 5 and Fig. 6.

In Figs. 8, the more complex case for the river Gauja and its tributary Vildoga is shown. In Fig. 8(a), the incomplete incisions of LAMO1 are presented.

At the place of incisions, the thickness of the Q2 aquifer is 1.0 meter and 0.02 meter for each of fifteen layers which are present above Q2 (relh, aer) and between the Q2 and D3am layers (gQ2z, Q1#, gQ1#z, …,D3pl, D3amz). The task of arranging the *z*-maps even for the incomplete incisions was complex and the effect of the full incisions of river valleys was still unknown.

Therefore, only the Quaternary layers Q2 and gQ2z were cut out by river valleys for the LAMO1 version.
It was necessary to develop more advanced software that could rearrange the *z*-surfaces at locations of the complete incisions [5].

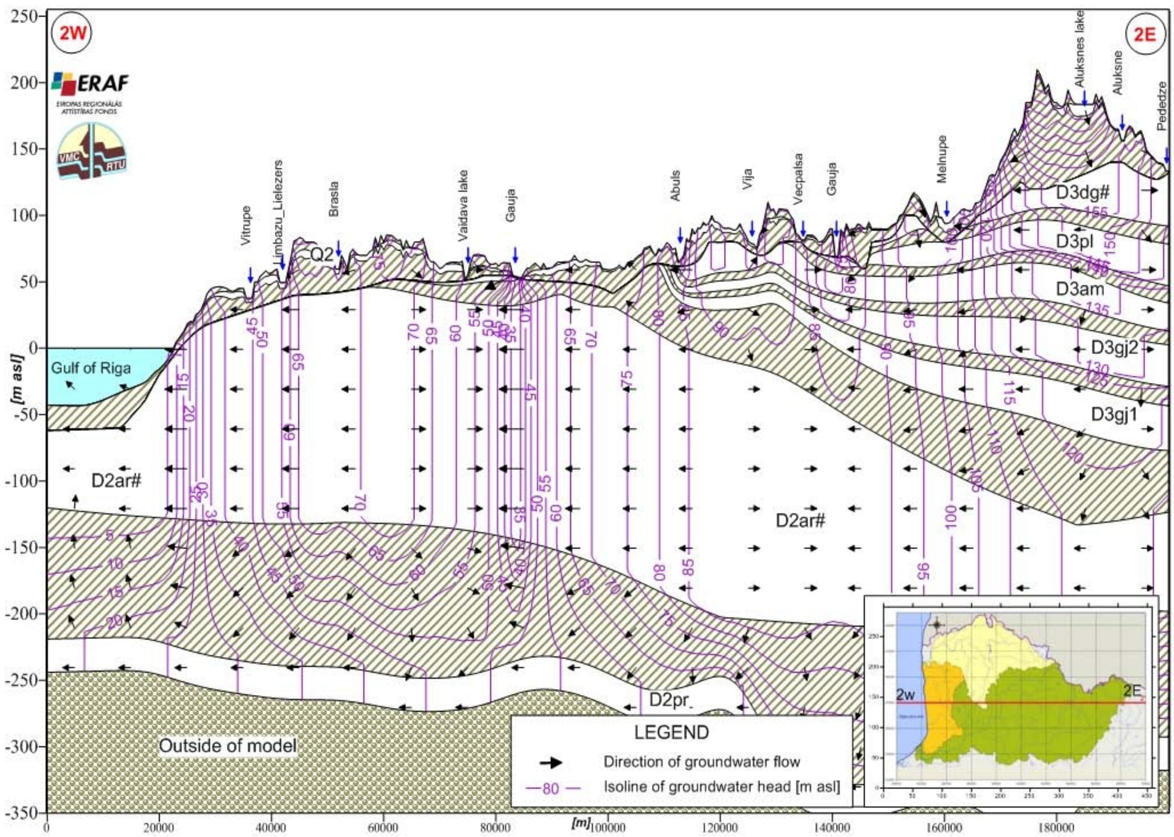

Fig. 5. Groundwater head isolines of the section 2W-2E for LAMO1

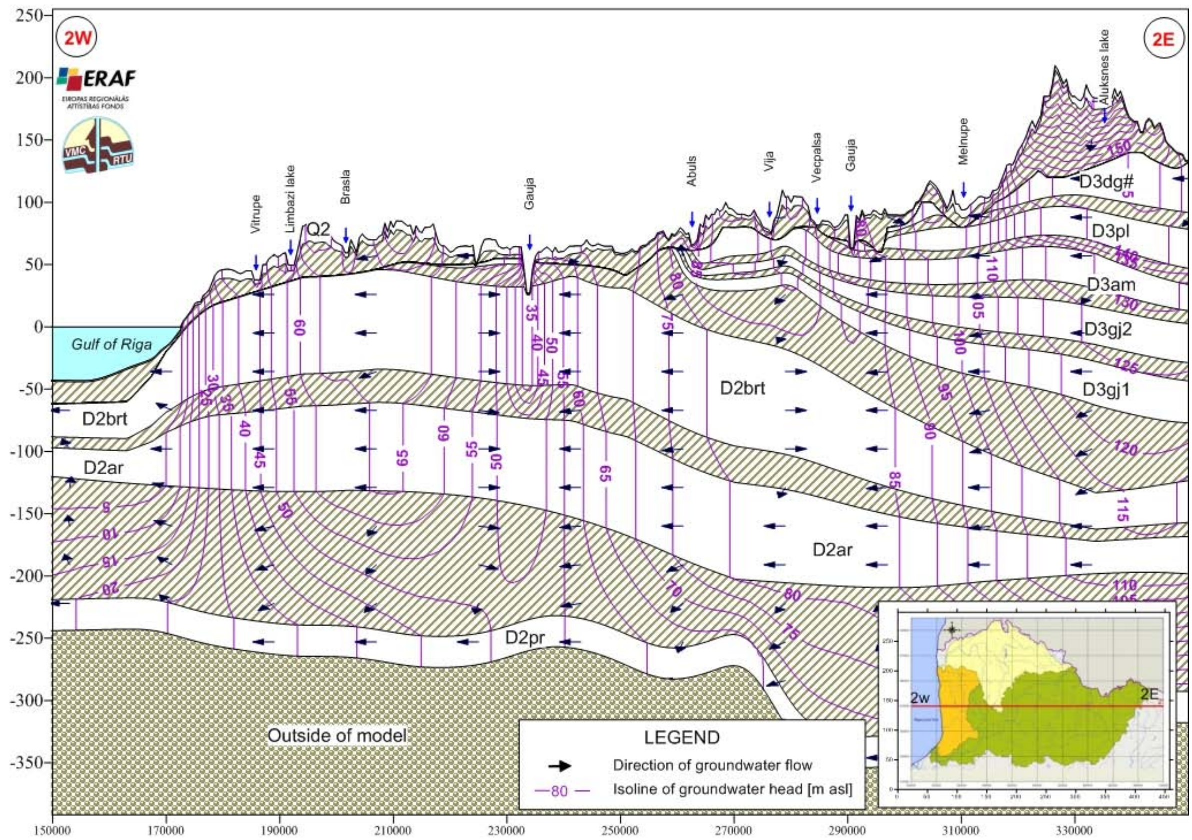

Fig. 6. Groundwater head isolines of the section 2W-2E for LAMO2

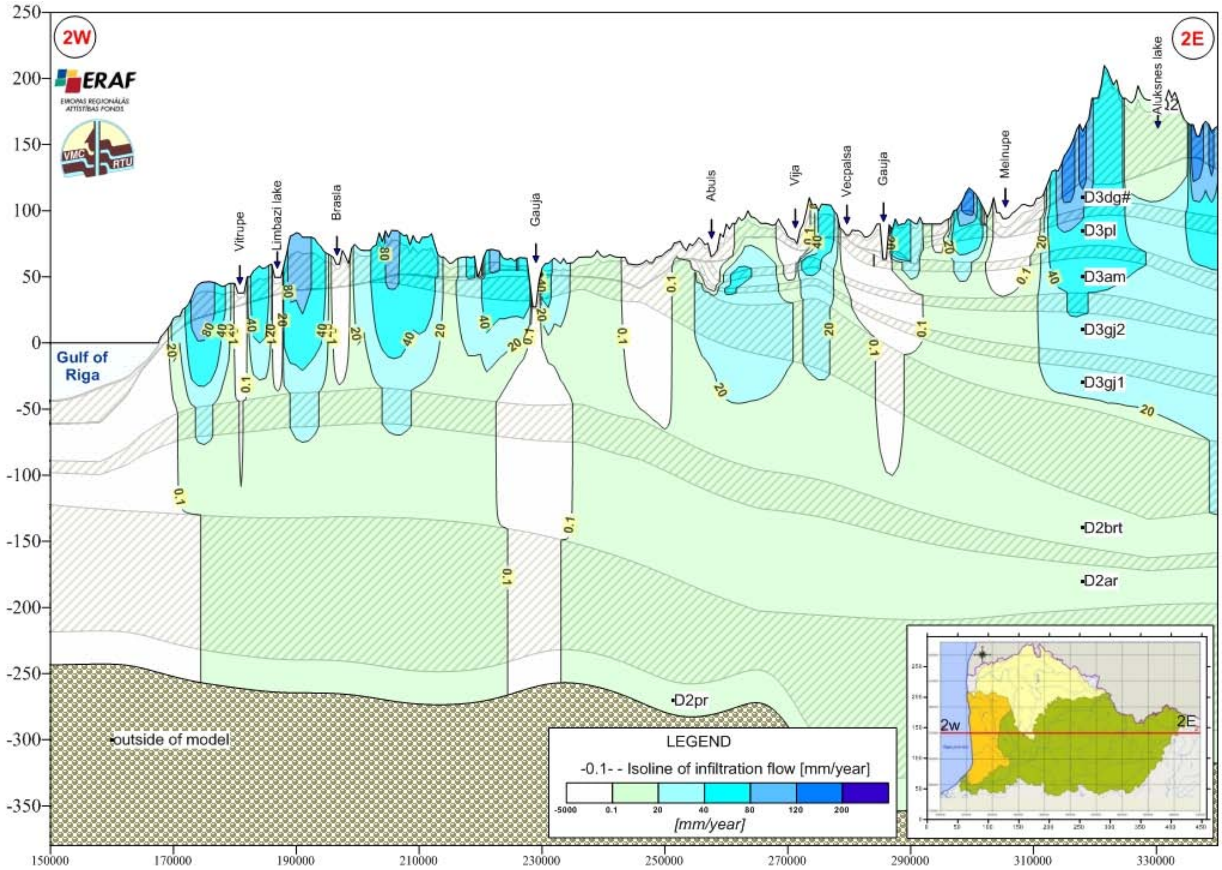

Fig. 7. Map for infiltration flow of the section 2W-2E of LAMO2

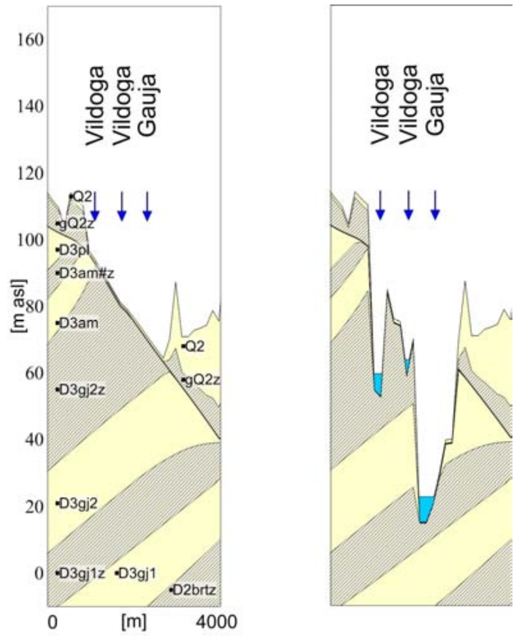

(a) LAMO1 (b)LAMO2

Figs. 8. Incisions of valleys for the Gauja river and its tributary Vildoga

In Fig. 8(b), the complete incisions of the river valleys are shown. There the geometry of the primary geological layers D3am, D3gj2z, D3gj2, D3gj1z is also changed and the ground surface of river valleys is simulated much more correctly.

IV. LAMO3 Upgrades

In 2014, LAMO2 has been turned into LAMO3: the transmissivity maps of primary aquifers were refined; the density of the HM hydrographical network was increased.

IV.1. Refinement of Transmissivity Maps

The transmissivity T for aquifers is very important, because it controls the groundwater motion there. For aquitards, $T = a_{xy} \sim 0$, because their permeability k is very small.

The transmissivity of aquifers can be measured in a variety of ways: field tests, laboratory tests, methods based on grain size distributions [10]. Inverse problem solving methods can also be applied [11]. However, the field tests where one pumping well is used are commonly applied. They permit the testing of large volumes of rock and they provide rather reliable data for finding transmissivity of aquifers. To improve the T-maps of LAMO3, well pumping data were applied.

The single well pumping test of the confined aquifer uses the discharge rate Q and the drawdown S of the groundwater head is observed. The test is presented by the expression [12]:

$$S = \frac{Q}{2\pi T}\left(ln\left(R/r\right)+\xi+\delta\right) \qquad T = k\,m \qquad (8)$$

where R and r are radiuses, accordingly, of the well depression cone and its screen; ξ and δ are additional hydraulic resistances that account for the partial penetrating factor of a well and for the quality of the well screen, respectively.

For a new well, $\delta = 0$. For old wells, the screen resistance δ increases and δ is unknown. For this reason, only pumping data of the new wells can provide reliable results and then $\delta = 0$ should be used in (8).

From (8), one can obtain:

$$T = \frac{v}{2\pi}\left(ln\left(R/r\right)+\xi\right), \qquad v = Q/S \qquad (9)$$

where v is the well specific capacity. If v and T have the dimensions [litre/(s.meter)] and [(meter)^2/day], respectively then:

$$T = 13.75v\left(ln\left(R/r\right)+\xi\right) \qquad (10)$$

Primary aquifers of LAMO are leaky and confined. Then $R = 1.12B$ [12]:

$$B = \sqrt{\frac{km}{k_1/m_1 + k_2/m_2}} \qquad (11)$$

where B is the leakage factor, $T = k\,m$ - transmissivity of the aquifer, k_1, m_1, and k_2, m_2 are permeability and thickness of the leaky confining aquitards, accordingly, located above and below the aquifer. In Table II, values of B, R and $ln(R/r)$ are given for a typical aquifer of LAMO when $r = (0.05 - 0.1)$ meter; k [meter/day]; B, R, m [meter].

TABLE II
COMPUTED VALUES OF *B*, *R*, *ln*(*R/r*)

km	k_1,k_2	m_1,m_2	*B*	*R*	*r*	*ln*(*R/r*)
200	10^{-4}	10	3162	3542	0.1	10.47
200	10^{-4}	5	2236	2504	0.1	10.12
200	10^{-4}	10	3162	3542	0.05	11.17
200	10^{-4}	5	2236	2504	0.05	10.82

By exploiting the fact that in Table II $ln(R/r) \sim 10.5$, one can approximate (10). If $\xi = 0$ then the following formula roughly provides the minimal value T_{min} of transmissivity for the confined aquifer:

$$T_{min} = 144\,v \qquad (12)$$

In [13], the following formula is presented for computing of ξ:

$$\xi = (1/a-1)(\ln 1.47ab-2.65a), \quad a = l/m, \quad b = m/r \qquad (13)$$

where m is the thickness of an aquifer and l and r are, accordingly, the length and radius of the well screen. The formula can be used if $m/r > 100$, $l/m \geq 0.1$. In Table III, the results given by (13) are presented.

TABLE III
VALUES OF WELL HYDRAULIC RESISTANCE ξ

l/m	m/r			
	100	200	500	1000
0.1	21.80	28.04	36.29	42.53
0.2	11.40	14.18	17.84	20.61
0.3	6.98	8.60	10.73	12.35
0.4	4.52	5.56	6.93	7.98
0.5	2.97	3.66	4.58	5.27
0.6	1.92	2.41	3.00	3.46
0.7	1.19	1.49	1.88	2.17
0.8	0.63	0.83	1.06	1.24
0.9	0.28	0.35	0.46	0.53
1.0	0.00	0.00	0.00	0.00

The resistance ξ can be applied, to refine the transmissivity *T*, as follows:

$$T = T_{min}\left(1+\xi/10.5\right) = cT_{min} \qquad (14)$$

For LAMO, the typical values of *l/m* and *m/r* are within the limits: 0.5 > *l/m* > 0.2; 500 > *m/r* > 100. Then, as it follows from Table III, the correction *c* may be within the limits: 2.8 > *c* > 1.3.

IV.2. Obtaining of Permeability Maps

The *k*-maps of permeability must be used to control the *T*-maps that are prepared by the GV system:

$$k = T/m \qquad (15)$$

where the transmissivity *T* is derived from the well pumping data; *m* is the aquifer thickness which is used in (3) by the GV system.

By using the EXCEL program [14], the set of the specific capacity *v* [litre/(s.meter)] must be extracted from the well pumping data. As a the rule, the *v*-set contains very low and also very high improbable values.

In order to normalize the set, minimal and maximal values of *v* are fixed (for LAMO3, v_{min} =0.3 and v_{max} =5).

The *v*-set contains *n* pointwise data. For LAMO, *n* > 1000 for all aquifers. Due to large *n*, the fast gridding method of "inverse distance to power" is applied by the SURFER program. This method computes the interpolated value σ_o at the node by using the available pointwise data $\sigma_i = 144\, v_i$, $i = 1,\ldots, n$, as follows [15]:

$$\sigma_o = \left(\sum_{i=1}^{n}\sigma_i\tau_i\right)/\sum_{i=1}^{n}\tau_i\,,\;\; \tau_i = \left(1/d_{oi}\right)^p$$
$$d_{oi} = \sqrt{\left(x_o - x_i\right)^2 + \left(y_0 - y_i\right)^2} \qquad (16)$$

where τ_i – the weight of σ_i; d_i – the distance between the grid node *o* and the σ_i point; *p* - the weighting power; x_o, y_o; x_i, y_i are coordinates, respectively, of the *o*-th grid node and the *i*-th point. The value $p = 2$ was used, to prepare σ_0 for LAMO3.

The interpolation result of (16) was rather rough and, to smooth it, the moving digital "inverse distance" low-pass filter of the size 11×11 (5km×5km area) was used [16]:

$$\sigma_{oo} = \left(\sum_{i,j}\sigma_{ij}\tau_{ij}\right)/\sum_{i,j}\tau_{ij}$$
$$\tau_{ij} = \left(1/D_{ij}\right)^p, \qquad D_{ij} = \sqrt{i^2 + j^2} \qquad (17)$$

where τ_{ij} – the filter weight; *p* - the power (*p* = 0.5 was applied); *i* and *j* were the grid row and column local indices for the neighboring nodes with respect to the central node *oo* of the filter; D_{ij} - the distance between the nodes *oo* and *ij*. In Table IV, the first quadrant of the τ_{ij} matrix of the filter (17) is shown. The filter contains four symmetrical quadrants, because negative *i* and *j* indices are also applied.

One can conclude from the values of τ_{ij} in Table IV that smoothing of the filter is moderate in comparison with the corresponding averaging filter where all weights τ_{ij} = 1.0. To preserve the data provided by wells, only one filtering pass was done.

The "inverse distance" interpolation and filtering do not account for discontinuity of aquifers that include the *m* = 0 areas. Thus, for all nodes of the 601 × 751 size grid of LAMO, values of T_{ij} are computed.

TABLE IV
WEIGHTS τ_{ij} FOR THE FIRST QUADRANT OF THE 11×11 SIZE FILTER

j						
5	0.444	0.443	0.431	0.414	0.395	0.376
4	0.500	0.492	0.473	0.447	0.420	0.395
3	0.577	0.562	0.527	0.485	0.447	0.414
2	0.707	0.669	0.595	0.527	0.473	0.431
1	1.000	0.841	0.669	0.562	0.432	0.443
0	2.000	1.000	0.707	0.577	0.500	0.444
	0	1	2	3	4	5 *i*

To obtain the *k*-map from the *T*-grid, the formula (15) must be used where the *m*-map of thickness is the divider. Only at the aquifer *m* > 0 area, reasonable *k* values can appear.

The extreme values of *k* that are caused by the dividers ε = 0.02 have to be replaced by the largest value $k_{\max}$ that can be found within the *m* > 0 area. The final *k*-map is obtained by applying the filter of (17).

IV.3. Increased Density of Hydrographical Network

In the versions LAMO1 and LAMO2, the 199 main rivers and the 67 largest lakes (area > 2.5km^2) of Latvia were included. However, the network of rivers of the country is much denser. To account for this feature, 469 rivers are simulated by LAMO3. The 270 "new" rivers are mostly tributaries of the "old" rivers (see Fig. 9).

The complemented set of rivers covers the land area of Latvia more evenly. Extra 60 small lakes (area > 1km^2) were also accounted for.

It was shown in [5] and in the next section, how the HM groundwater flows changed due to appliance of the much denser hydrographical network.

Fig. 9. Rivers and lakes of LAMO2 (blue color) and the new ones of LAMO3 (red color)

This network has also caused the necessity for appliance of the smaller plane approximation step *h* of HM:

- the bodies of rivers/lakes are somewhere located so close that their areas are touching;
- the HM area that are joined with rivers (~10 thous.km^2) is too large (the land area of Latvia is 64.5thous.km^2); the area decreases twofold when h = 500 → 250.

The both drawbacks will be eased in the next LAMO4 version.

V. Comparison of LAMO2 with LAMO3

The permeability maps and the groundwater flows of the both HM versions are compared.

V.1. Permeability Maps

For LAMO1 and LAMO2, constant values of *k* were used to compute the *T*-maps of primary aquifers. For this reason, *T* is in the direct proportion to the thickness *m* of an aquifer. For LAMO, the *k*-map is presented as the following product:

$$k = k_{norm}\, k_{mean}\,, \quad k_{norm} = k\,/\,k_{mean}$$
$$k_{mean} = \sum_{i=1}^{n} k_i \,/\, n \qquad (18)$$

where k_{norm} – the normalized *k*–map; k_{mean} and *n* - the mean value of *k* and the number of grid nodes at the $m > 0$ area, accordingly. For LAMO2, k_{norm} =1.0.

In Table V, the summary on features of the LAMO2 primary aquifers is presented. The aquifers differ in their areas, mean thicknesses m_{mean} and values of *k*. The mean transmissivity $T_{mean} = k\, m_{mean}$.

In Table VI, the main features of the LAMO3 primary aquifers are summarized. Their *k*-maps are variable (k_{max}/k_{min} >1). Minimal values of *T* are presented, because the resistances ξ are not accounted for.

The mean values of $(l/m)_{mean}$ are given for each aquifer. These values are smaller for the united aquifers D3ktl#, D3zg#, D3krs#, D3dg#.

TABLE V
SUMMARY ON FEATURES OF LAMO2 PRIMARY AQUIFERS

Aquifer code	Area [thous.km^2]	m_{mean} [meter]	T_{mean} [meter^2/day]	m_{max}/m_{min} $=T_{max}/T_{min}$	*k* [meter/day]	k_{max}/k_{min}
D3ktl#	5.44	62.89	188.67	7772.5	3.0	1.00
D3zg#	7.53	50.43	151.29	4382.0	3.0	1.00
D3krs#	9.34	22.71	45.42	2253.0	2.0	1.00
D3dg#	32.84	30.76	307.60	4437.5	10.0	1.00
D3pl	44.10	22.98	229.80	2840.5	10.0	1.00
D3am	46.52	22.11	221.10	2269.0	10.0	1.00
D3gj2	51.17	26.55	265.50	2924.0	10.0	1.00
D3gj1	56.66	31.79	445.06	4287.5	14.0	1.00
D2brt	68.96	45.30	226.50	5520.5	5.0	1.00
D2ar	68.96	41.00	205.00	4904.0	5.0	1.00

It follows from Table V and Table VI that the k_{mean} and T_{mean} values of the deeper aquifers D3pl, D2gj2, D3gj1, D2brt, D2ar are considerably smaller for LAMO3. This resulted in decrease of groundwater flows there [5].

The ratio T_{max}/T_{min} is much larger for LAMO2, because there the ratio depends only on the *m*-maps.

In the next LAMO4 version, the research on improving the T-maps will continue. The effect of the resistance ξ will be accounted for individual wells, the initial data will be checked more carefully in order to exclude the faulty ones. The method that accounts for the *m*=0 areas will be improved.

TABLE VI
SUMMARY ON FEATURES OF LAMO3 PRIMARY AQUIFERS

Aquifer code	T_{mean} [meter^2/day]	T_{max}/T_{min}	k_{mean} [meter/day]	k_{min} [meter/day]	k_{max} [meter/day]	k_{max}/k_{min}	$(l/m)_{mean}$
D3ktl#	82.66	2675.0	2.12	0.50	4.50	9.00	0.15
D3zg#	125.38	2062.5	3.64	1.50	8.00	5.33	0.24
D3krs#	121.17	1315.0	5.95	2.30	10.00	4.35	0.36
D3dg#	127.82	2370.0	5.58	0.70	10.00	14.38	0.34
D3pl	156.11	1158.0	6.11	1.78	15.15	8.51	0.55
D3am	94.87	1247.0	4.69	1.50	8.50	5.67	0.53
D3gj2	136.00	1410.0	5.58	2.20	10.00	4.55	0.49
D3gj1	145.62	1220.0	5.24	1.60	10.00	6.25	0.51
D2brt	79.03	1843.0	1.91	0.60	3.50	5.83	0.40
D2ar	80.64	1662.5	2.13	0.65	4.00	6.15	0.50

V.2. Flows of LAMO2 and LAMO3

To compare the groundwater flow regimes of LAMO2 with LAMO3, Table VII, Table VIII, Table IX and Table X were prepared. Table VII and Table VIII contain the groundwater flow balances of Latvia that were obtained by LAMO2 and LAMO3.

For an aquifer, the GV system computes the flows q_{topin}, q_{topout}, q_{botin}, q_{botout}. Their sum is the inflow q_{inflow}:

$$q_{inflow} = q_{topin} + q_{topout} + q_{botin} + q_{botout} \qquad (19)$$

The flow q_{inflow} exists only for the $m > 0$ area of a layer. The GV system also finds the flows q_{river}, q_{lakes}, q_{border} and q_{wells}, accordingly, for rivers, lakes, external boundaries and exploitation wells.

The sum of these flows must be in balance with q_{inflow}:

$$q_{inflow}+q_{river}+q_{lakes}+q_{border}+q_{wells} = 0 \qquad (20)$$

The graphical scheme for the expressions (19) and (20) is given by Fig. 10(a) and Fig. 10(b), correspondingly. There a "module" represents any part of the geological environment which flow balance is under consideration.

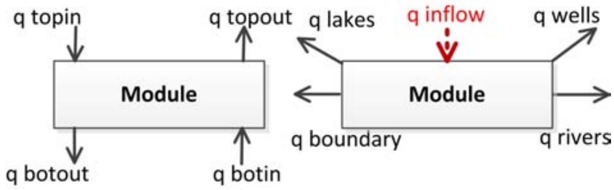

(a) sources of inflow (b) local balance

Figs. 10. Scheme for explanation of flow balance

TABLE VII
LATVIA GROUNDWATER FLOWS [THOUS. M^3/DAY] FOR LAMO2

Aquifer code	q_{inflow}	q_{rivers}	q_{lakes}	q_{border}	q_{wells}
Q2	3888	-3288	-426	-118	-56
Q1#	25	-7	0	-18	0
D3ktl#	173	-192	0	20	-1
D3zg#	63	-41	0	-18	-4
D3krs#	23	-11	0	-8	-4
D3dg#	599	-569	-10	-15	-5
D3pl	516	-446	8	-70	-8
D3am	144	-93	0	-50	-1
D3gj2	365	-244	0	-96	-25
D3gj1	505	-327	0	-154	-24
D2brt	689	-462	0	-214	-13
D2ar	209	0	0	-195	-14
Model	7199	-5680	-428	-936	-155
Q1+Q2	3913	-3295	-426	-136	-56
Primary aquifers	3286	-2385	-2	-800	-99

An aquifer is the smallest module, but any HM or its parts can also be modules (Fig. 11 and Fig. 12).

In Table VII and Table VIII, the local flow balance is given for any aquifer, for whole HM, for the Quaternary and Primary strata systems. In Fig. 11, the last three rows of Table VIII are exposed. In Table IX, the flow difference of LAMO3 and LAMO2 are shown (Table VII was subtracted from Table VIII). The last three rows of Table IX are exposed by Fig. 12.

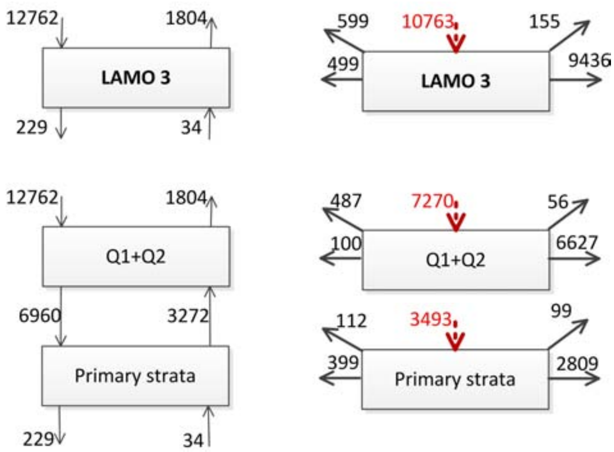

Fig. 11. Mass balances [thous. m^3/day] for LAMO3

It follows from Table IX that the total inflow for LAMO3 has increased by 3564 thous.m^3/day, the flows of rivers and lakes have the enlargements 3756 thous.m^3/day and 171 thous.m^3/day, accordingly.

The LAMO2 version was calibrated to match the total river flow ~ 6000 thous.m^3/day given in [17]. For LAMO3, the total river flow is much larger than for LAMO2 (9436 > 5680).

This difference is mostly due to the Quaternary system (6627 > 3295) where nearly all "new rivers" of LAMO3 are joined.

TABLE VIII
LATVIA GROUNDWATER FLOWS [THOUS. M3/DAY] FOR LAMO3

Aquifer code	q_{inflow}	q_{rivers}	q_{lakes}	q_{border}	q_{wells}
Q2	7223	-6596	-487	-84	-56
Q1#	47	-31	0	-16	0
D3ktl#	261	-277	0	17	-1
D3zg#	82	-64	-3	-11	-4
D3krs#	94	-80	0	-10	-4
D3dg#	800	-692	-90	-13	-5
D3pl	474	-361	-8	-97	-8
D3am	262	-237	0	-24	-1
D3gj2	527	-443	0	-59	-25
D3gj1	322	-213	-5	-80	-24
D2brt	557	-442	-6	-96	-13
D2ar	114	0	0	-100	-14
Model	10763	-9436	-599	-499	-155
Q1+Q2	7270	-6627	-487	-100	-56
Primary aquifers	3493	-2809	-112	-399	-99

At present, it is not clear if the simulated river flows in LAMO3 are not much larger than in nature. The right answer will be possible when the measurements of river flows will be accounted for by the next LAMO4 version.

The effect of the "new" lakes is little, because their areas are small (1km^2-2.5km^2). The 110 thous.m^3/day increase for the Primary system is caused mainly by the artificial lakes of hydroelectric-power stations of the Daugava river. These lakes are joined with the D3dg# and D3pl aquifers (Table VIII and Table IX).

In Table X, the infiltration flows γ [mm/year] are computed for LAMO2 and LAMO3, if the $m > 0$ areas of aquifers are accounted for:

$$\gamma = 0.365\, q_{inflow} / L \tag{21}$$

where L [thous.km^2], q_{inflow} [thous.m^3/day], accordingly, are the area of an aquifer (Table V) and its inflow q_{inflow} which is taken from Tables VII and VIII for LAMO2 and LAMO3, respectively.

For LAMO3, the flow through boundaries was smaller by 363=(936–499) thous.m^3/day. This decrease was caused mainly by the Primary strata system (327 thous.m^3/day), because there, for the deeper D3gj2, D3gj1, D2brt, D2ar aquifers, the k_{mean} values were smaller than the ones of LAMO2 (Table V and Table VI). It follows from Table X that for LAMO3, the mean infiltrations (L = 64.5 thous.km^2) on the HM top and of the Quaternary system are larger (60.91 > 40.73) and (41.14 > 22.14) mm/year, correspondingly.

TABLE IX
GROUNDWATER FLOW [THOUS. M^3/DAY] DIFFERENCE BETWEEN LAMO3 AND LAMO2

Aquifer code	Δq_{inflow}	Δq_{rivers}	Δq_{lakes}	Δq_{border}	Δq_{wells}
Q2	3335	-3308	-61	34	0
Q1#	22	-24	0	2	0
D3ktl#	88	-85	0	-3	0
D3zg#	19	-23	-3	7	0
D3krs	71	-69	0	-2	0
D3dg#	201	-123	-80	2	0
D3pl	-42	85	-16	-27	0
D3am	118	-144	0	26	0
D3gj2	162	-199	0	37	0
D3gj1	-183	114	-5	74	0
D2brt	-132	20	-6	118	0
D2ar	-95	0	0	95	0
Model	3564	-3756	-171	363	0
Q1+Q2	3357	-3332	-61	36	0
Primary aquifers	207	-424	-110	327	0

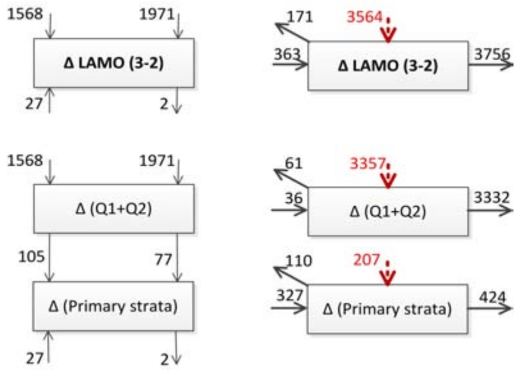

Fig. 12. Flow difference [thous. m3/day] between LAMO3 and LAMO2

TABLE X
INFILTRATION FLOW FOR LAMO2 AND LAMO3

Aquifer code	Area [thous.km^2]	γ [mm/year] LAMO2	γ [mm/year] LAMO3
D3ktl#	5.44	11.61	17.71
D3zg#	7,53	3.05	3.97
D3krs	9.34	0.90	3.67
D3dg#	32.84	6.66	8.89
D3pl	44.10	4.27	3.92
D3am	46.52	1.13	2.05
D3gj2	51.17	2.60	3.76
D3gj1	56.66	3.25	2.07
D2brt	63.40	3.96	3.20
D2ar	63.40	1.20	0.66
Primary Total	-	38.63	49.90
Model	64.50	40.73	60.91
Q1+Q2	64.50	22.14	41.14
Primary aquifers	64.50	18.59	19.76

For the Primary strata, if the real areas are used, the flows are larger than the mean ones: for LAMO2 (38.63 > 18.59) and for LAMO3 (49.90 > 19.76) mm/year. The mean infiltration of LAMO3 is only slightly larger (49.90 > 19.76) mm/year than the one for LAMO2.

VI. Next Upgrades

In 2015, LAMO3 will be converted into LAMO4 where the plane approximation step will be reduced from 500 meters to 250 meters. In LAMO3, bodies of rivers/lakes are somewhere touching. In LAMO4, due to use of the smaller approximation step, this problem will be eased, hence the ground surface will be simulated with the higher accuracy.

Rivers will be joined with the HM body more trustworthy, because the data of the river flows will be accounted for. The research on improving the *T*-maps will continue. In the near future, LAMO4 may also be used for complex geochemical studies, because the GV system can simulate migration of various groundwater ingredients in space and time as described in [18], [19] where HM of Lithuania has been used. LAMO is in close relationship with this model, because the RTU team has participated in its development [20]. Methods and results described in [18], [19] are very instructive for users of LAMO.

VII. Conclusion

The case of improving the hydrogeological model of Latvia LAMO has been considered.

The upgrades have improved credibility of the main LAMO results: the groundwater head and flow distributions, geological stratigraphy data, permeability of geological layers and etc. The next LAMO4 version will be applied for updating information that is necessary for water management planning, as the base for creating detailed local models and for investigation of complex geochemical processes.

Acknowledgements

In 2010-2012, the hydrogeological model of Latvia LAMO1 has been developed within the framework of the Riga Technical University project that was co-financed by the European Regional Development Fund.

The current upgrades of LAMO3 and LAMO4 are supported by the Latvian State Research program EVIDEnT.

References

[1] Water Framework Directive. 2000. (2000/60/EC of the European Parliament and of the Council). *Official Journal of the European Communities,* L327, 22.12.2000.

[2] Environmental Simulations, Inc., Groundwater Vistas. Version 6, Guide to using, 2011.

[3] Spalvins, A., Slangens, J., Lace, I., Aleksans, O., Krauklis, K., Efficient methods used to create hydrogeological model of Latvia, (2013) *International Review on Modelling and Simulations (IREMOS),* 6 (5), pp. 1718-1726.

[4] A. Spalvins, J. Slangens, I. Lace, K. Krauklis, and O. Aleksans, Survey of the first results provided by hydrogeological model of Latvia. *In Conference Proceedings 9-th International Conference Environmental Engineering, (22-23 May, 2014, Vilnius, Lithuania), Vilnius Gediminas Technical university Press Technika, ISBN 978-609-457-690-4 CD , ISSN 2029-7092 online*

[5] A. Spalvins, J. Slangens, I. Lace, K. Krauklis, V. Skibelis, O. Aleksans, and I. Eglite, Hydrogeological model of Latvia after increasing density of its hydrographical network, *Scientific Journal of Riga Technical University, Boundary Field Problems*

and Computer Simulation, vol. 53, pp. 12-24, 2014, Available http://www.emc.rtu.lv
[6] Mapping of groundwater bodies of the Gauja-Koiva river basin district., *Report on contract carried out by Riga Technical University, 25-maps, (in Latvian), 2013, [Online]. Available:* http://www.emc.rtu.lv/ .
[7] G. Strang, *Linear algebra and its applications*.(Academic Press Inc., New York, p., 373, 1976)
[8] J. Bear, *Hydraulics of groundwater*, (McGraw Hill Inc., Israel, 567 p., 1979)
[9] Golden Software, Inc., *SURFER-11 for Windows, Users manual*, Guide to Using, 2012
[10] P. A. Domenico, and F.W. Schwartz. *Physical and Chemical Hydrogeology*.,(John Wiley and sons, Inc. – 2 end ed. New York, p. 506,1998)
[11] Y.C. Chin, Application of differential evolutionary optimization methodology for parameter structure identification in groundwater modelling, *Hydrogeology Journal, Volume 22, Number 8, December 2014, pp. 1731-1748*
[12] N. Bindeman, and I. Jazvin, *Evaluation of Groundwater Resources*. (Moscow: Nedra, 1982 (in Russian)).
[13] N. Verigin, *Methods Used for Finding Permeability of Geological Strata*, (Moscow: Gosstroiizdat, 1962 (in Russian)).
[14] J. Walkenback, *Excel-7 Bible*. (Indianapolis, Wiley Publishing, Inc., 2007)
[15] R. Franke, Scattered Data Interpolation: Test of Some Methods, *Mathematics of Computations, vol.33, pp. 181-200, 1982.*
[16] I. Ditas, Digital Image Processing Algorithms and Applications, (New York: John Wiley and Sons, 2000).
[17] I. Dzilna,. *Resources, composition and dynamics of groundwater for the middle part of the Baltic area*. (Zinatne, Riga, 1970, p. 197, (in Russian)).
[18] R. Mokrik, V. Juodkazis, A. Stuopis, and J. Mazeika, Isotope geochemistry and modelling of the multi-aquifer system in the eastern part of Lithuania. In *Hydrogeology journal.*, Vol. 22, 2014, pp. 925-941,.
[19] A. Stuopis, *Formation and modelling assessment peculiarities of the Quaternary aquifer system groundwater resources in the southeastern part of Lithuania*. (Summary of doctoral dissertation, Vilnius university, Natural research centre, Vilnius, 2014, p. 58.).
[20] A. Spalvins, J. Slangens, I. Lace, A. Stuopis, A. Domasevicius, Creating of Regional Hydrogeological Model for the South-East of Lithuania. In: *Proceedings of XXXVIII IAH Congress Groundwater Quality Sustainability, Extended Abstracts (CD). Poland, Krakow, September 12-17, 2010, pp. 1233-1238.*

Authors' information

Aivars Spalvins was born in Latvia. In 1963 he graduated from Riga Polytechnical Institute (Riga Technical University since 1990) as a Computer Engineer. He is Head of the Environment Modeling Centre of Riga Technical University. His research interests include computer modeling of groundwater flows and migration of contaminants.
E-mail: emc@cs.rtu.lv

Janis Slangens was born in Latvia. In 1969 he graduated from Riga Polytechnical Institute (Riga Technical University, since 1990) as a Computer Engineer. He is a Senior Researcher with the Environment Modeling Centre of Riga Technical University. His research interests include computer modeling of groundwater flows.
E-mail: janis.slangens@rtu.lv

Inta Lace was born in Latvia. In 1971 she graduated from Riga Polytechnical Institute (Riga Technical University, since 1990) as a Computer Engineer. In 1995 she received a Master's Degree in Applied Computer Science. Since 1991 she is a Researcher with the Environment Modeling Centre of Riga Technical University.
E-mail: intalace@yahoo.com

Olgerts Aleksans was born in Latvia. In 1979 he graduated from Vilnius State University as a Hydrogeologist & Engineering Geologist. In 2011 he received a Doctor's Degree in Geology. Since 2011 he is a Researcher with the Environment Modeling Centre of Riga Technical University.
E-mail olgerts.aleksans@gmail.com

Kaspars Krauklis received a Master's Degree in Computer Systems from Riga Technical University in 2007 and the Certificate in Teaching of Engineering Sciences from the Institute of Humanities of Riga Technical University in 2005. Presently he is a Researcher with the Environment Modeling Centre of Riga Technical University.
E-mail: kasparskrauklis@gmail.com

International Review on Modelling and Simulations (IREMOS)

(continued from outside front cover)

Abstracting and Indexing Information:

Academic Search Complete - EBSCO Information Services
Cambridge Scientific Abstracts - CSA/CIG
Elsevier Bibliographic Database SCOPUS
Index Copernicus (Journal Master List): ***Impact Factor 6.55***

Autorizzazione del Tribunale di Napoli n. 78 del 1/10/2008

Praise Worthy Prize

1974-9821(201504)8:2;1-N